Nonlinear Kinematics for Improved Helicopter Tracking

E J Clark, E J Griffith, S Maskell, J F Ralph
Department of Electrical Engineering and Electronics,
University of Liverpool,
Liverpool, England.
{ejclark, e.griffith, smaksell, jfralph} @liverpool.ac.uk

***Abstract*—This paper compares the tracking performance that can be achieved when using a nonlinear drag model for a helicopter, a constant drag motion model, and a baseline constant acceleration model. A particle filter is used for state estimation to address problems associated with nonlinear drag and nonlinear measurements of helicopter pose. We demonstrate that the inclusion of this nonlinear kinematic effect provides improved tracking performance for a manoeuvring target.**

Keywords—Target tracking; State estimation; Helicopter motion model; Particle filters.

I. INTRODUCTION

With the growth of interest in autonomous vehicles and robotics, there is an increasing need for automatic tracking systems that take noisy sensor data and extract accurate motion information. The output has a number of possible uses, from collision avoidance and general situational awareness to military applications in war-fighting and defensive systems. In each of these areas, the ability to provide accurate track data in a timely manner reduces the risks associated with ambiguous and often confusing sensor measurements.

In this paper, we consider tracking applications for improved air defense based on nonlinear motion models for helicopters. The aim is to demonstrate the use of nonlinear kinematic models to enhance the accuracy of tracking systems for short-range air defense engagements, where the target may be manoeuvring. Modern short-range air defense systems often rely on a fixed sensor and tracking system to provide commands to a high velocity interceptor. Typically, commands are provided via radar or laser systems – either as semi-active guidance (an interceptor with a forward looking sensor picking up reflected energy from the target) or a beam-riding system (a rear-facing sensor picking up energy directly from the command tracker). For stationary or slow moving targets, maintaining a beam riding or designator signal on the target is relatively straightforward. However, for fast moving or manoeuvring targets, maintaining a single aim point is more challenging. Further, to maximize the effectiveness of the interceptor, it may not be sufficient to keep the aim-point within the target outline and achieve a 'hit'. It may be necessary to identify vulnerable locations within the target and to maintain the aim point on this location. Future air defense systems relying on high-powered lasers would eliminate the need for an interceptor, but they do not remove the need for accurate tracking and pointing systems. For maximum effectiveness, such systems also require that the laser energy is concentrated on small vulnerable areas of the target. The requirement to provide high accuracy, real-time target track data will remain as one of the main drivers for air defense applications.

This paper is organized as follows. Section II describes previous work in using aircraft orientation to infer manoeuvre information to assist in tracking and state estimation. Section III introduces the three motional models considered in this paper and the measurements used by the three different models. Section IV describes the state estimation processes used to filter the measurements for the three models. Section V shows the results from an example scenario, where a helicopter is flying towards a sensor and manoeuvring repeatedly. The results show the benefits found using the nonlinear drag and nonlinear measurement model. Section VI summarizes the work and draws conclusions about the possible benefits of the approach described in the paper.

II. BACKGROUND

The target tracking problem has been tackled with numerous types of linear and nonlinear filters such as the Kalman filter [1], its modifications [2,3], and the many guises of the particle filter [4,5]. Although these filters can be used to great effect, their effect can be improved if we use them in conjunction with information about the target's intention. Li and Jilkov [6] have noted that even when a model for a manoeuvring target is accurate, the control system either remains unknown or is lacking in information, identifying a potential source for error in the estimated state. When an aircraft manoeuvres, it has to change something about its behavior in order to effect that change. For example, if an aircraft is to gain height, it is likely to increase its angle of attack. If it is to increase speed in straight and level flight, it will likely increase its thrust, but to maintain straight and level flight, it will also have to pitch down slightly. Measurement of these aspects of the aircraft's state enables a tracker to know something about how the aircraft might manoeuvre and this then starts to bound the probability associated with the future state. The ability to measure and estimate the attitude or the 'pose' of the aircraft should therefore assist in tracking the aircraft as it manoeuvres. This is the main subject of this paper, as applied to the problem of tracking helicopter targets.

The Kalman filter has been used to show an improvement in performance when the attitude of an aircraft is measured [7]. However, the motion of a tracked aircraft is often nonlinear, especially when manoeuvring. A Kalman filter, being linear, will not represent the complete range of possible manoeuvres and it is unlikely to provide the full benefit of such an approach. To address this, we have chosen to use a nonlinear particle filter [4,5]. There are many aspects to the nonlinearity of a manoeuvring aircraft, because the acceleration of an aircraft is rarely, if ever, precisely linear. Even when in straight and level flight, an autopilot will make small changes to correct for the turbulence around the aircraft body. The requirement for modeling such motion has been considered previously. For example, Yang et al. focus on this ability [8] using the Unscented transform [3] to deal with their nonlinearities. The Unscented transform provides speed and computational efficiency for a tracking system with nonlinear measurements, but in exchange it can reduce the robustness of the system. Andrisani et al. [9] have reported problems in using measurements of a helicopter's main rotor plane due to the small angles involved. If these angles could be measured accurately, then the conclusions may have been more favorable. However, there are always limits to such measurements and it is often difficult to measure small changes in attitude or pose when the target is relatively small and not fully resolved by the sensor. The resultant uncertainties can therefore be large and this can lead to instabilities or a lack of robustness in the state estimates. A robust system that includes these uncertainties in an accurate description of aircraft motion and the measurement process is therefore favorable. To provide this robustness, we will use a manifestly nonlinear tracker, a particle filter [4,5].

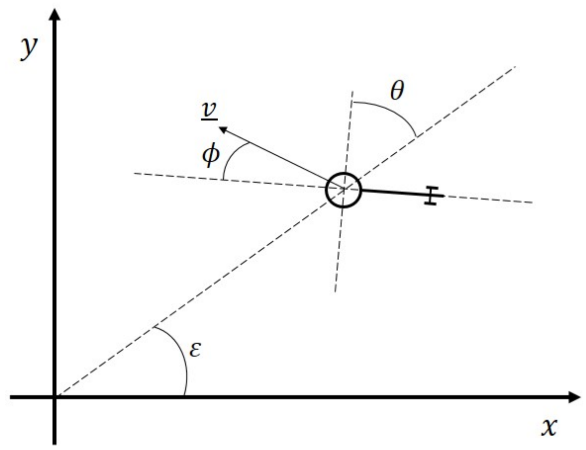

Fig. 1. Geometry showing sensor axes, helicopter orientation and velocity vector.

III. Helicopter Motion Models

The main aim of the paper is to compare the accuracy of a tracker using three different kinematic models for the motion of a helicopter target. The three models are: a baseline nearly-constant acceleration model (using simple linear kinematics); a kinematic model that includes a constant drag term (an acceleration that is proportional to the velocity and acts against the current motion); and a nonlinear drag model (where the drag is a nonlinear function of the angle between the velocity vector and the longitudinal body axis, which is determined from a measurement of helicopter pose). We restrict the analysis to a horizontal 2D engagement for simplicity, but the extension to three dimensions is a straightforward generalization. The geometry is defined in Fig.1, where the angles are: the sensor line of sight angle from the x-axis (denoted by ε), the pose angle showing the alignment of the aircraft to the line of sight (denoted by θ, θ = 0 being broadside (90º) to the line of sight), and the angle between the longitudinal aircraft axis and the velocity vector, sideslip (denoted by ϕ).

A. Baseline Constant Acceleration Model

As a baseline for comparison, we will use a standard linear kinematic model with nearly-constant acceleration, and a standard process noise model to allow for small variations in the actual acceleration of the target. The state vector for this model contains position, velocity and acceleration, and is given by,

$$\underline{X}_A = (x \quad v_x \quad a_x \quad y \quad v_y \quad a_y)^T \tag{1}$$

where the co-ordinates (x,y) are in an earth-stabilised/sensor reference frame. The linear kinematics are represented by the matrix,

$$\underline{F}_A = \begin{pmatrix} 1 & \Delta t & \frac{1}{2}(\Delta t)^2 & 0 & 0 & 0 \\ 0 & 1 & \Delta t & 0 & 0 & 0 \\ 0 & 0 & 1 & 0 & 0 & 0 \\ 0 & 0 & 0 & 1 & \Delta t & \frac{1}{2}(\Delta t)^2 \\ 0 & 0 & 0 & 0 & 1 & \Delta t \\ 0 & 0 & 0 & 0 & 0 & 1 \end{pmatrix} \tag{2}$$

where,

$$\underline{X}_A(t+\Delta t) = \underline{F}_A \cdot \underline{X}_A(t) + \underline{\Gamma} \cdot \underline{v}(t) \tag{3}$$

$\nu(t)$ is an acceleration noise source, with standard deviation denoted by σ_a, where

$$\underline{\Gamma} = \begin{pmatrix} \frac{1}{2}(\Delta t)^2 & 0 \\ \Delta t & 0 \\ 1 & 0 \\ 0 & \frac{1}{2}(\Delta t)^2 \\ 0 & \Delta t \\ 0 & 1 \end{pmatrix} \tag{4}$$

and the process noise covariance is given by the discrete Wiener process acceleration model [2].

$$\underline{Q} = \begin{pmatrix} \frac{1}{4}(\Delta t)^4 & \frac{1}{2}(\Delta t)^3 & \frac{1}{2}(\Delta t)^2 & 0 & 0 & 0 \\ \frac{1}{2}(\Delta t)^3 & (\Delta t)^2 & \Delta t & 0 & 0 & 0 \\ \frac{1}{2}(\Delta t)^2 & \Delta t & 1 & 0 & 0 & 0 \\ 0 & 0 & 0 & \frac{1}{4}(\Delta t)^4 & \frac{1}{2}(\Delta t)^3 & \frac{1}{2}(\Delta t)^2 \\ 0 & 0 & 0 & \frac{1}{2}(\Delta t)^3 & (\Delta t)^2 & \Delta t \\ 0 & 0 & 0 & \frac{1}{2}(\Delta t)^2 & \Delta t & 1 \end{pmatrix} \cdot \sigma_a^2 \tag{5}$$

B. Constant Drag Motion Model

The second kinematic model includes the effect of drag on the motion of the helicopter, but – without information regarding the pose of the aircraft – it does so in the simplest possible way by taking the average of the actual drag function over all possible values of sideslip (i.e. all values for the angle ϕ). The model is the same as the baseline model described above with, $\underline{X}_B = \underline{X}_A, \underline{Y}_B = \underline{Y}_A$ etc., with a different kinematic matrix,

$$\underline{F}_B = \begin{pmatrix} 1 & \Delta t - \frac{\alpha}{2}(\Delta t)^2 & \frac{1}{2}(\Delta t)^2 & 0 & 0 & 0 \\ 0 & 1-\alpha(\Delta t) & \Delta t & 0 & 0 & 0 \\ 0 & 0 & 1 & 0 & 0 & 0 \\ 0 & 0 & 0 & 1 & \Delta t - \frac{\alpha}{2}(\Delta t)^2 & \frac{1}{2}(\Delta t)^2 \\ 0 & 0 & 0 & 0 & 1-\alpha(\Delta t) & \Delta t \\ 0 & 0 & 0 & 0 & 0 & 1 \end{pmatrix} \quad (6)$$

where α is the average value for the drag coefficient.

Strictly, this model should require a different process noise covariance matrix to the simple baseline case. It is more properly represented as an integrated Ornstein–Uhlenbeck process [10]. However, as long as the drag coefficient and/or the time step is small enough for $\alpha(\Delta t) << 1$ then any corrections to the standard process noise will be negligible [10], and we will use the process noise matrix $\underline{Q}$ above in each of the cases for simplicity.

C. Nonlinear Drag Motion Model

The nonlinear drag model is developed to represent the manoeuvreability of a helicopter in all forms of flight (in the horizontal plane in our 2D example): forward, sideways, and backwards. The characteristics of helicopter flight are such that the maximum acceleration of the aircraft in each direction is approximately equal ($a_{max}(\phi) = a_{max}$) but the maximum speed in each direction is dependent on the angle of flight relative to the longitudinal axis. The maximum speed achievable is greatest for forward motion (along the longitudinal axis) and falls rapidly to the side or to the rear. To represent these properties, we model the differences in terms of an angle dependent drag coefficient ($\alpha = \alpha(\phi)$) which gives an angle dependent maximum speed ($v_{max} = v_{max}(\phi)$). In particular, we use a hyperbolic secant function to model the angular dependence with,

$$\alpha(\phi) = \frac{a_{max}}{v_{max}(\pi)} + \left(\frac{a_{max}}{v_{max}(0)} - \frac{a_{max}}{v_{max}(\pi)}\right)\mathrm{sech}\left(\frac{\phi}{\Delta\phi}\right) \quad (7)$$

where $\Delta\phi$ controls the width of the cone where the forward speed is a maximum. An example is shown in Fig.2. To allow this angular dependence to be included in the kinematic model, it must be possible to estimate the pose of the helicopter to obtain the angle between the longitudinal axis of the aircraft and the velocity vector. An estimate for the velocity vector is already contained in the state vector given above, but to estimate the pose an estimate of the angle θ is also required. We therefore augment the state vector by adding the pose angle,

$$\underline{X}_C = (x \quad v_x \quad a_x \quad y \quad v_y \quad a_y \quad \theta)^T \quad (8)$$

For this system, the kinematics are nonlinear functions of ϕ, which is – in turn – a nonlinear function of the pose angle (θ) and the velocity vector.

$$\begin{aligned} x(t+\Delta t) &= x(t) + (\Delta t)\cdot v_x(t) + \tfrac{1}{2}(\Delta t)^2 \cdot (a_x(t) - \alpha(\phi)v_x(t)) \\ v_x(t+\Delta t) &= v_x(t) + (\Delta t)\cdot(a_x(t) - \alpha(\phi)v_x(t)) \\ a_x(t+\Delta t) &= a_x(t) \\ y(t+\Delta t) &= y(t) + (\Delta t)\cdot v_y(t) + \tfrac{1}{2}(\Delta t)^2 \cdot (a_y(t) - \alpha(\phi)v_y(t)) \\ v_y(t+\Delta t) &= v_y(t) + (\Delta t)\cdot(a_y(t) - \alpha(\phi)v_y(t)) \\ a_y(t+\Delta t) &= a_y(t) \\ \theta(t+\Delta t) &= \theta(t) \end{aligned} \quad (9)$$

where θ is assumed to be approximately constant. The process noise $\underline{Q}$ is the same as in the previous two cases, although the matrix is augmented with an extra row and column for the pose angle, θ, with variance $(\sigma_\theta)^2$ and uncorrelated with the rest of the noise.

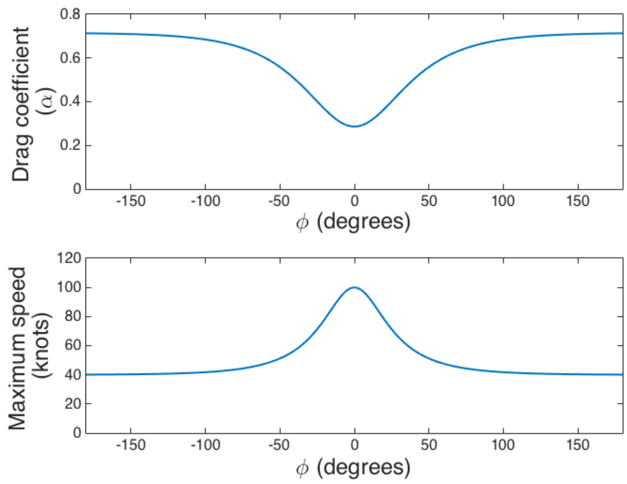

Fig. 2. Example of nonlinear drag function and maximum speed as functions of the angle ϕ between the longitudinal body axis and the velocity vector.

D. Measurements

For the baseline model (A) and the constant drag model (B), the measurement is a direct measurement of the co-ordinates so

$$\underline{Y}_A = \underline{H}\cdot \underline{X}_A + \underline{r}_A = \begin{pmatrix} x \\ y \end{pmatrix} + \underline{r}_A \quad (10)$$

where $\underline{r}_A$ is measurement noise and the measurement noise covariance is given by

$$\underline{R}_A = \begin{pmatrix} \sigma_x^2 & 0 \\ 0 & \sigma_x^2 \end{pmatrix} \quad (11)$$

where we have defined equal measurement errors in x and in y, and a simple sensor model to concentrate on the effect of the motion models and not to confuse the analysis with sensor specific factors.

The measurement for the third motion model (C) includes a measurement of the pose angle. For this, we assume that an imager can resolve the helicopter sufficiently for the relative position of the different parts of the airframe (main rotors, engine and/or tail rotors) to be distinguished. The ability to resolve the main components of the airframe gives some information about the orientation of the aircraft relative to the line of sight of the sensor. However, this is not a direct measurement of the pose angle since there is an ambiguity as to whether the aircraft is angled towards or away from the sensor. As a result, the measurement is a measurement of |θ| rather than θ. Therefore, the measurement is also a nonlinear function with measurement noise $\underline{r}_C$.

$$\underline{Y}_C = H(\underline{X}_C, \underline{r}_C) = \begin{pmatrix} x + r_{C1} \\ y + r_{C2} \\ |\theta + r_{C3}| \end{pmatrix} \tag{12}$$

where the measurement noise covariance is given by

$$\underline{R}_C = \begin{pmatrix} \sigma_x^2 & 0 & 0 \\ 0 & \sigma_x^2 & 0 \\ 0 & 0 & \sigma_\vartheta^2 \end{pmatrix} \tag{13}$$

where $(\sigma_\vartheta)^2$ is the variance of the pose angle.

IV. State Estimation – Particle Filter

At the heart of any target tracking system is a state estimation process. It filters a sequence of noisy sensor measurements and produces a target track, consisting of a sequence of filtered states or state vectors representing the best estimates for the target motion. For the three motion models that we will be considering, the first (baseline) model (A) is entirely linear and the acceleration is assumed to be constant (up to the perturbative effect of a random Gaussian process noise). This means that a Kalman filter [1] is sufficient for this example, but a more complex state estimation technique is required for the more complex motion models: constant drag (B), and nonlinear drag with nonlinear pose measurements (C). For these two examples, we choose a particle filter [5], and – for simplicity – we choose the 'bootstrap filter' [4,5], which provides a means to model the effect of the nonlinearities on the system but does not lead to too onerous an implementation. In each case, the measurements are used to update and refine estimates of the target location, velocity and acceleration, and target pose in the case of filter C.

A particle filter, or a Sequential Monte Carlo (SMC) filter [5], is a method for estimating probability distributions. It works by generating large numbers of sample points and weighting. The sample points are referred to as 'particles' and each particle corresponds to a vector in the state space for the system. Estimates for the statistical parameters are found by performing a weighted sum over all the particles rather than integrating over the (unknown) distribution. The bootstrap filter is a particle filter where the particles are weighted according to the probability of obtaining each measurement given the state vector that is attached to that particle. The closer the state vector is to the true underlying state, the larger the weight that should be attached to it over a sequence of measurements.

More formally, we take an initial set of sample vectors in the appropriate state space (six dimensional in the case of filter B and seven dimensional in the case of filter C). The initial weights for each vector are set to be equal, $w_i(0) = 1/n_p$ for all i, where i runs from 1 to n_p, the number of particles. For the examples shown below, the number of sample vectors (particles) was varied between $n_p = 1000$ and $n_p = 4000$, although $n_p = 4000$ was used for the results shown in the figures. Once an initial set of sample points has been selected, each sample point evolves independently under the action of the motion model described in the appropriate section above for one time step. The weight for each particle is then updated according to

$$w_i(t+\Delta t) = w_i(t) \cdot g(\underline{Y}(t) | \underline{X}(t)) \tag{14}$$

where $g(\underline{Y}|\underline{X})$ is referred to as the likelihood – the probability of obtaining a measurement $\underline{Y}$ given that the system is in state $\underline{X}$. In our case, these distributions are Gaussian and are given by

$$g(\underline{Y}(t)|\underline{X}(t)) \propto \exp\left(\frac{(Y_1 - X_1)^2}{2\sigma_x^2}\right) \cdot \exp\left(\frac{(Y_2 - X_4)^2}{2\sigma_x^2}\right) \tag{15}$$

for filter B and

$$g(\underline{Y}(t)|\underline{X}(t)) \propto \exp\left(\frac{(Y_1 - X_1)^2}{2\sigma_x^2}\right) \cdot \exp\left(\frac{(Y_2 - X_4)^2}{2\sigma_x^2}\right) \cdot \exp\left(\frac{(Y_3 - |X_7|)^2}{2\sigma_\vartheta^2}\right) \tag{16}$$

for filter C, including the distribution in the pose angle, θ. This last distribution contains an approximation, because the angular variable cannot strictly be represented by a Gaussian distribution, but in the cases contained in this paper the differences between this and the correct distribution are negligible. We have also selected a prior kernel that only considers the current state of the system provided by the particle – giving the 'bootstrap filter'. More complicated kernels could be selected, which consider the history of the track associated with each particle, but for the purposes of this paper we have selected the simplest case which still encapsulates the nonlinearities and produces accurate state estimates.

Once the individual particle weights have been updated, the particle weights are then normalized. Over a sequence of time steps, the weights attached to some particles reduce and others increase. To avoid a small number of particles gaining too much weight, a resampling step is used to remove the particles with low weight (low probability) and increase the number of high weight particles. To avoid doing this at each timestep, a simple check is used to calculate the effective number of particles N_{eff} [5],

$$N_{eff} = \left(\sum_i w_i^2\right)^{-1} \tag{17}$$

When this value falls below a fixed threshold (normally set to be $n_p/2$ [5]) then the particles are resampled. In the simplest case, as used here, the cumulative probability distribution function is constructed and new particles are selected uniformly from this distribution, so that particles with large weights are more likely to be selected but even those with relatively small weights still have some probability of being represented in the new resampled set of particles. The resampled particles have the state vector inherited from their 'parent' particle and all are allocated the same weight. As the system evolves – with particle evolution, particle reweighting, and an occasional resampling – the distribution of particles within state space should provide an approximation for the underlying probability distribution and estimates can be obtained for the state vector, calculated from a weighted mean over all particles.

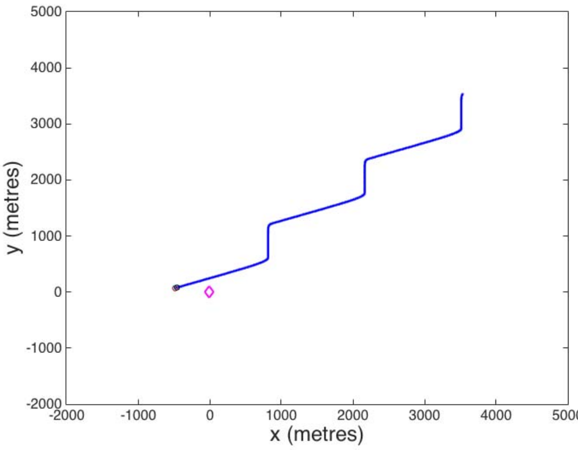

Fig. 3. Example trajectory for manoeuvring helicopter scenario. Sensor shown as diamond at origin, helicopter trajectory approaching the sensor shown as solid line.

V. Results – Manuevering Targets

As an example, we consider a case where the target is moving towards the sensor and making deliberate evasive manoeuvres and changing the pose angle by changing between flying forwards and sideways (ϕ = 0º and ϕ = 90º) at each manoeuvre point. The manoeuvres are set at 30 second intervals. The speed, the direction of flight and the drag characteristics change after each manoeuvre. The example shown in Fig. 3 is a helicopter travelling at 100 knots forwards (ϕ = 0º), and a maximum of 40 knots sideways (ϕ = 90º) and using the drag characteristics shown in Fig. 2. The sensor measurement noise has a standard deviation of σ_x = 20 metres, and the standard deviation for the pose angle measurement noise is chosen to be σ_ϑ = 10º. The other parameters are fixed to be: a_{max} = 1.5g, $\Delta\phi$ = 30º, σ_θ = 2º, σ_a = 0.1g.

In Fig. 4, the average (RMS) position errors are shown. Between the manoeuvres, the accuracy of the estimated positions for the two particle filters is better than that of the simple Kalman filter but both show a similar performance. There is a slight benefit in using the nonlinear drag model (C) when the helicopter is flying sideward (0-30 seconds, 60-90 seconds, and 120-150 seconds). The main differences are found during the manoeuvres themselves. The peak RMS error values during a manoeuvre are 14.7 metres, 16.8 metres and 12.0 metres for the constant acceleration, constant drag and nonlinear model respectively. The performance of the constant drag model deteriorates significantly during the transitions from forwards flight to sideways flight (at 60 seconds and 120 seconds).

The Kalman filter shows a similar performance for all manoeuvres and exhibits a slight lag as the filter adjusts to the new motion. The nonlinear drag model provides good performance throughout.

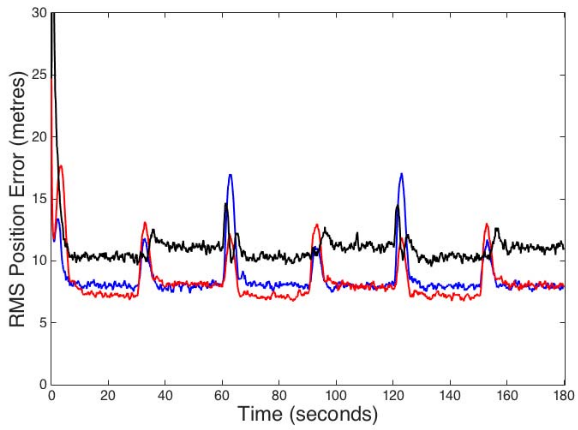

Fig. 4. RMS position errors for manoeuvring helicopter scenario shown in Fig. 3. Black curve is filter A (baseline Kalman). Blue curve is filter B (constant drag model). Red curve is filter C (nonlinear drag model).

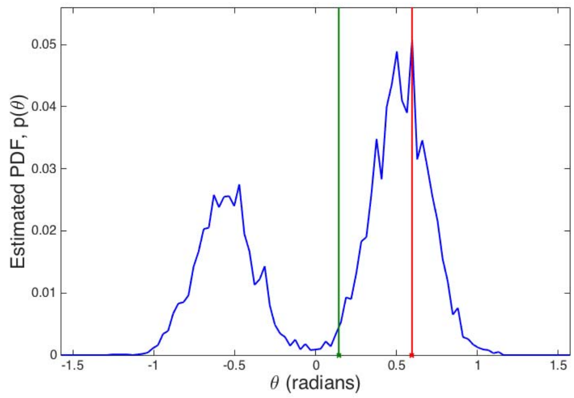

Fig. 5. Example multi-model estimated probability density function for helicopter pose angle (θ) for filter C (nonlinear drag model). Average (estimated) value for pose angle shown in green, and the actual pose angle in red.

Fig. 5 shows an example of the estimated probability density function (pdf) for the target pose angle, θ, which is clearly seen to be multi-model, with peaks at +/− the true value. Although the pdf is often single modal and approximately Gaussian in shape during steady flight, it tends to become multi-modal when the target is manoeuvring, and the fact that the pdf can be multi-model is a good justification for the use of the particle filter to represent the nonlinear measurement in this case.

VI. Discussion and Conclusions

In this paper, we have considered a target tracking example where knowledge of the orientation of the target can be used to improve the accuracy of the tracker. The example selected was for a helicopter, where the aircraft may manoeuvre to move in different directions with the aircraft oriented forwards, sideways or backwards. We have described the kinematics of the aircraft using a 2D nonlinear motion model, although this may be readily generalized to three-dimensional problems. The problem also gives rise to a nonlinear measurement. The sensor is assumed to be able to determine the relative displacement of major components of the airframe (engines, exhaust, main rotors, etc.). However, this leaves an ambiguity over the exact orientation so that the pose of the aircraft may still be unclear. The aircraft may be turned towards the sensor or turned away but still show the same relative displacement. This ambiguity was found to lead to multi-modal distributions in the estimated pose angle, which are best dealt with using a particle filter or similar SMC method. Standard Kalman based methods do not have the flexibility to represent this type of distribution.

Using an example scenario, we have demonstrated that the inclusion of this nonlinear kinematic model and measurement of pose, together with a particle filter for state estimation, can improve the tracking accuracy relative to a baseline Kalman filter or a constant drag model with no knowledge of the aircraft pose. The accuracy of the nonlinear motion model was found to be better overall than the baseline near-constant acceleration model using a Kalman filter, and it was found to represent target manoeuvres more accurately than the constant drag model.

The particle filter used in this paper was a relatively straightforward bootstrap filter, which uses a simple form for the proposal distribution – one which is based on the current state estimate only. Extensions of this work to consider more sophisticated forms of proposal distribution, realistic sensor models, and alternative motion models (incorporating realistic manoeuvres) are likely to show further benefits in terms of track accuracy.

ACKNOWLEDGEMENTS

This work was supported by an EPSRC Industrial CASE award and by Thales UK (Belfast).

REFERENCES

[1] R.E. Kalman, A new approach to linear filtering and prediction problems. Journal of basic Engineering, 82(1), pp.35-45, 1960.

[2] Y. Bar-Shalom, X.R. Li, and T. Kirubarajan, The Extended Kalman Filter. In: Estimation with Applications to Tracking and Navigation. John Wiley & Sons, pp.381-394, 2004.

[3] S.J. Julier, and J.K. Uhlmann, July. New extension of the Kalman filter to nonlinear systems. In AeroSense'97 (pp. 182-193). International Society for Optics and Photonics, 1997.

[4] N. J. Gordon, D. J. Salmond, A. F. M. Smith, "Novel approach to nonlinear/non-Gaussian Bayesian state estimation." in IEE Proceedings F (Radar and Signal Processing), vol. 140, no. 2, pp. 107-113, 1993.

[5] M. S. Arulampalam, S. Maskell, N. Gordon and T. Clapp, "A tutorial on particle filters for online nonlinear/non-Gaussian Bayesian tracking," in IEEE Transactions on Signal Processing, vol. 50, no. 2, pp. 174-188, Feb 2002.

[6] X.R. Li, and V.P. Jilkov, Survey of manoeuvring target tracking. Part I. Dynamic models. IEEE Transactions on aerospace and electronic systems, 39(4), pp.1333-1364, 2003.

[7] D. Andrisani, F. P. Kuhl and D. Gleason, "A Nonlinear Tracker Using Attitude Measurements," in IEEE Transactions on Aerospace and Electronic Systems, vol. AES-22, no. 5, pp. 533-539, Sept. 1986.

[8] R. Yang, G.W. Ng, and Y. Bar-Shalom. "Bearings-only tracking with fusion from heterogenous passive sensors: ESM/EO and acoustic." Information Fusion (Fusion), 2015 18th International Conference on. IEEE, 2015.

[9] D. Andrisani, E. T. Kim, J. Schierman and F. P. Kuhl, "A nonlinear helicopter tracker using attitude measurements," in IEEE Transactions on Aerospace and Electronic Systems, vol. 27, no. 1, pp. 40-47, Jan 1991.

[10] S. Maskell, "Sequentially Structured Bayesian Solutions", PhD thesis, Cambridge University Engineering Department, 2004.